ORIGINAL ARTICLE

Multi-objective process parameter optimization considering minimum thermal accumulation on spindles of dry hobbing machine

Bo Li[1] · Yanbin Du[1,2] · Xiao Yang[1,2] · Guohua He[1] · Lang He[1]

Abstract

The thermal accumulation problem of the dry hobbing machine spindles is quite serious and is an essential reason for gear machining accuracy. Hence, this study focuses on thermal accumulation modeling and optimization for dry hobbing machine spindles. Firstly, the thermal accumulation characteristics of the hob spindle and workbench spindle in dry hobbing machine are clarified, and the effect mechanism of thermal accumulation on the machine spindles deformation is revealed. Then, the thermal accumulation models for the hob spindle and workbench spindle in dry hobbing machine are established, respectively, and the characteristic parameters of the thermal accumulation models are quantitatively analyzed. Finally, a multi-objective optimization approach for the process parameters considering minimum thermal accumulation in dry hobbing machine spindles is proposed, and a case study is conducted. The experimental results indicate that the thermal accumulation of the hob spindle and workbench spindle is reduced by 11.17% and 19.3%, respectively; the hobbing efficiency is increased by 8.22% as well as effectively reducing the average temperature of the machine spindles and controlling the gear's M-value, which proves the effectiveness of proposed approach.

Keywords Dry hobbing · Spindle · Thermal accumulation model · Multi-objective optimization

1 Introduction

Dry cutting is a green and advanced manufacturing technology with the advantages of high productivity, low machining cost, and low environmental hazards in the workshop [1–3]. However, the high speed and absence of cutting oil/liquid cooling lubrication for dry hobbing machine result in higher heat production than heat dissipation in the machine spindles, which eventually leads to significant thermal deformation problems [4, 5]. It is worth noting that the spindles of dry hobbing machine are located in a separate confined cutting space, which dramatically limits the heat dissipation from spindles and enhances the thermal accumulation effect of spindles. Therefore, studying the thermal accumulation models and their optimization approaches in dry hobbing

machine spindles is of great theoretical significance and practical value for improving gear machining accuracy.

According to the current research results, thermal deformation errors account for 40 to 70% of the total error in the machine, which is the leading cause of the impact on workpiece machining accuracy [6]. To investigate and mitigate the thermogenic effects of the machine tool, Zhang et al. [7] derived and established the thermal error transfer function of the whole machine, and combined it with time and frequency domain analysis to obtain the machine's thermal characteristics. Zhao et al. [8] established a thermal analysis model for identifying large EDM machines' static and dynamic thermal behavior, and revealed the heat balance characteristics of the machines. Yao et al. [9] proposed an approach for modeling heat errors in machine tools based on dynamic temperature gradients and optimized the location of temperature measurements on the machine. Feng et al. [10] theoretically analyzed the thermal and temperature distribution characteristics of machine screw shafts, and proposed a new model based on thermal characterization to compensate for positioning errors. Wei et al. [11] proposed a thermal error prediction model based on Gaussian process regression, which enables interval thermal error

✉ Yanbin Du
 dyb@ctbu.edu.cn

1 Chongqing Key Laboratory of Manufacturing Equipment Mechanism Design and Control, Chongqing Technology and Business University, Chongqing 400067, China

2 Chongqing Machine Tool (Group) Co., Ltd, Chongqing 400055, China

prediction for machine tools. Narendra et al. [12] developed a real-time thermal error compensation module for precision machine tools, which has been successfully implemented on a diamond turning machine. The above studies are feasible and effective in analyzing and mitigating the thermogenic effects of conventional machine tools. However, dry hobbing machines differ from conventional machine tools in terms of structure, heat source, and heat dissipation, resulting in very complex thermal characteristics and thermal deformation mechanisms. Hence, there are limitations to the study of heat problems on dry hobbing machines that require further exploration.

Due to the uniqueness and complexity of the heat flow characteristics and temperature field distribution in dry hobbing machine, the thermal impact problem has received extensive attention. Zhu et al. [13] analyzed the heat accumulation characteristics of dry hobbing machine and established a multivariable heat control model to effectively control the variation of temperature and heat deformation error for machine components. Kadashevich et al. [14] proposed an improved DEXEL model to visualize the gear's geometric features and temperature field. Li et al. [15] conducted thermal-structural coupling numerical simulations of the heat transfer process and thermal deformation on dry hobbing machine workbench, and revealed the temperature field distribution characteristics of workbench. Yang et al. [16] revealed the heat accumulation mechanism for dry hobbing machines and established a heat balance optimization model, which effectively reduced the average temperature in the machine cutting space. Li et al. [17] analyzed the thermal energy accumulation characteristics of the hob spindle in dry hobbing machine and established a thermal energy balance optimization model for the electric spindle system based on process parameters. However, the above studies have focused on the thermal characteristics and thermal effects of a single component in dry hobbing machine, leaving a gap in research into the simultaneous implementation of thermal balance regulation for multiple key components. Therefore, this study plans to conduct synergistic analysis of the thermal accumulation characteristics of the hob spindle and workbench spindle in dry hobbing machine. Based on the above ideas, the authors' team has already conducted some related studies on the thermal problems of dry hobbing machine, such as the heat flow characteristics of dry hobbing machine [18], the generation of cutting heat [19], and the thermal deformation effects of hot chips on the workbench [20], which provide some basis for the subsequent thermal accumulation optimization of the machine spindles.

The thermal accumulation of the dry hobbing machine spindles directly affects the gear machining quality and is closely related to the dry hobbing process parameters. On the one hand, the process parameters determine the machine heat source's thermal generation and the cooling system's

heat dissipation efficiency, which further affects the thermal accumulation of the spindles. On the other hand, the thermal accumulation control optimization of a single machine spindle will have local optimum solutions, which have limitations for improving the workpiece accuracy. Therefore, in this study, the thermal accumulation models of the hob spindle and workbench spindle in dry hobbing machine are established to obtain the process parameters that minimize the thermal accumulation of the machine.

The detailed research structure of this study is as follows: Section 2 clarifies the thermal deformation mechanism of the spindles for dry hobbing machine; Section 3 establishes the thermal accumulation model of the dry hobbing machine spindles; Section 4 establishes the multi-objective optimization model of minimum thermal accumulation for machine spindles; Section 5 conducts a case study on multi-objective optimization approach of process parameters for minimum thermal accumulation in dry hobbing machine spindles; Section 6 summarizes the research and looks ahead to subsequent studies.

2 Thermal deformation mechanism of dry hobbing machine spindles

Dry hobbing machine has many differences from conventional machine tools, including structural characteristics, cooling methods, etc. As shown in Fig. 1a and b, compared to wet hobbing machines, the inside in dry hobbing machine consists of a separate enclosed cutting space with machine shields, metal covers, and isolation baffles. In addition, dry hobbing is high-speed machining and adopts compressed air instead of cutting oil/fluid, resulting in enormous heat generation and extremely ineffective heat dissipation of the machine spindles. As shown in Fig. 1a and c, compared with other metal cutting machine tools, the dry hobbing machine has two spindles, including the hob spindle and workbench spindle, and they are forced to mesh and rotate according to the transmission ratio in hobbing process. The forced meshing of the two spindles exacerbates the generation of cutting heat and causes coupling effects on thermal deformation of the hob spindle and workbench spindle. Therefore, the heat flow characteristics and thermal deformation mechanism of dry hobbing machine spindles have their own complexity and specificity.

The heat flow in the dry hobbing machine spindles consists of three forms. One is the heat transfer to air through thermal convection; the second is the heat transfer to the directly contacted components by heat conduction; the third is the heat radiation to the surrounding area. Dry hobbing machine spindles are directly driven by two separate servo motors; the hob spindle and workbench spindle are subject to heat transfer from the motors by heat conduction and heat

Fig. 1 Structural characteristics comparison of dry hobbing machine

(a) Dry hobbing machine　(b) Wet hobbing machine　(c) Vertical milling machine
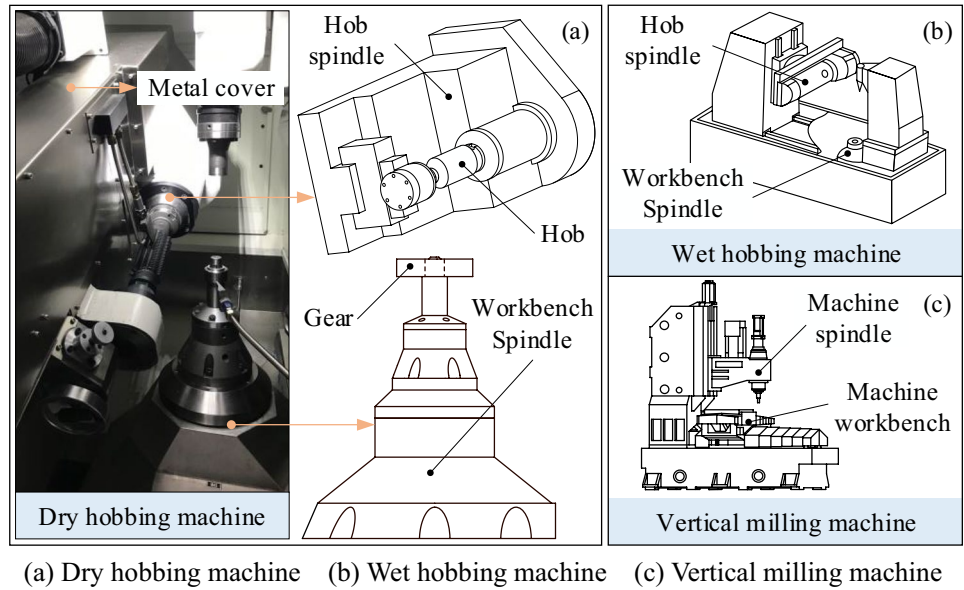
radiation. Gears and bearings are the common kinematic pairs of the hob spindle and workbench spindle; the machine spindles will be subject to heat conduction and heat radiation from the gears and bearings. In addition, due to the close proximity of the hob spindle to feed system, it is also subject to heat conduction and heat radiation from ball screws, guides, etc.. Cutting heat is one of the main heat sources for the machine spindles, in which small part is transferred to the spindles through hob and workpiece. The majority is carried away from the machine by cooling air and hot chips. It is worth noting that hot chips are subject to heat conduction and heat radiation with workbench spindle in the discharge process. The environment temperature and electronic components can also have some effect on the heat flow of machine spindles through heat convection and heat

radiation. The heat transfer model for dry hobbing machine spindles is shown in Fig. 2.

The unequal heat generation and heat dissipation in dry hobbing machine spindles will lead to thermal accumulation effects, resulting in uneven distribution of its temperature field and thermal deformation, which in turn causes deviations in the cutting amount and cutting position of the workpiece material and impacts the gear machining accuracy. As shown in Fig. 3, the black model represents the shape of the machine spindles before machining, and the red model represents the shape of the machine spindles during the machining process when thermal deformation occurs. Dry hobbing machine spindles after the thermal accumulation effect will result in heat deformation so that they become skewed. Hob deviates δ_{wx}, δ_{wy}, δ_{wz} in the X, Y, and

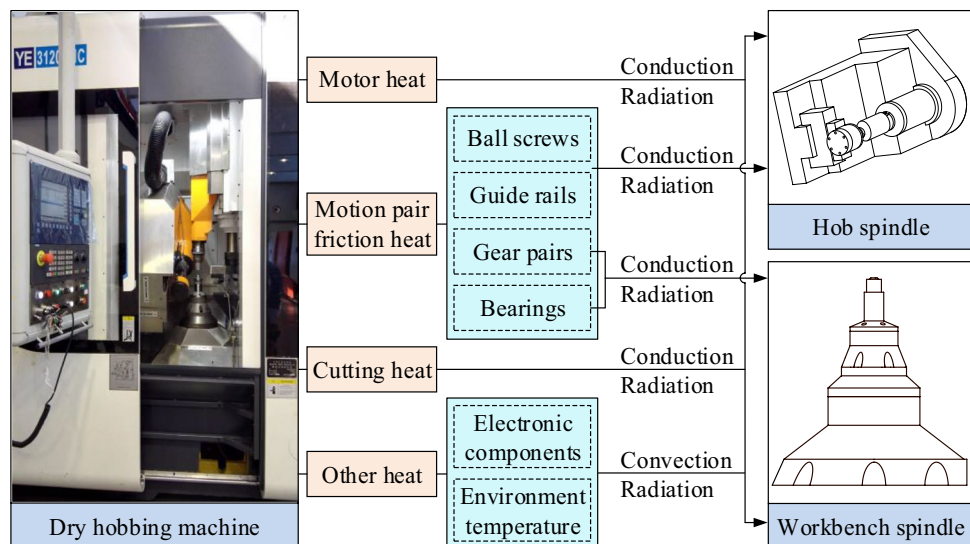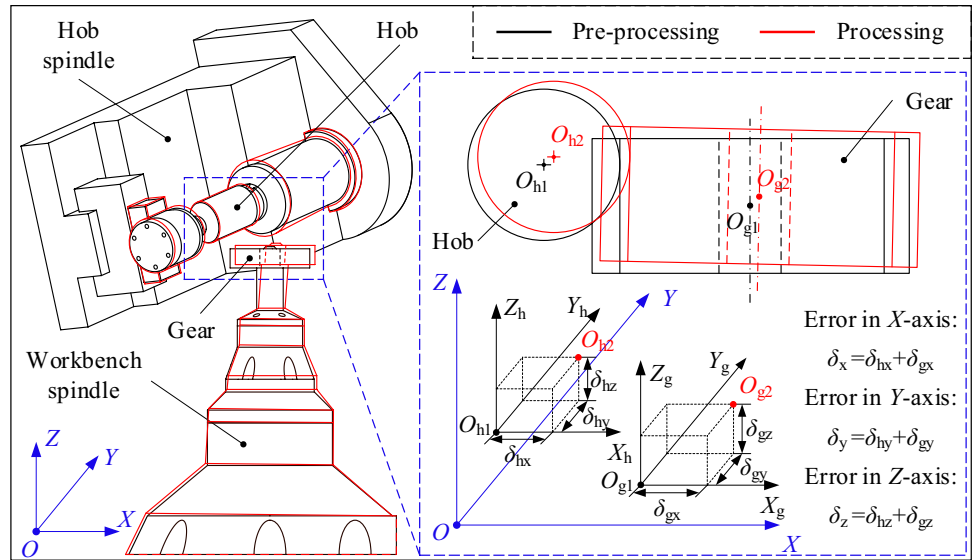**Fig. 2** Heat transfer model of dry hobbing machine spindles

Fig. 3 Thermal deformation mechanism of dry hobbing machine spindles

Z directions, respectively; workpiece deviates δ_{wx}, δ_{wy}, δ_{wz} in the X, Y, and Z, directions, respectively, which together constitute the thermal deformation error of gear machining. It is worth emphasizing that the thermal deformation error $\delta_x = \delta_{hx} + \delta_{wx}$ in the X direction has the greatest impact on the hobbing accuracy. Therefore, the temperature rise of the hob spindle and workbench spindle can be reduced by controlling their thermal accumulation, thus decreasing δ_{hx}, δ_{wx}, respectively, to minimize the thermal deformation error δ_x of gear in the X direction.

The research on the thermal control of guide rails, ball screws, motors, and gear pairs is quite mature. Meanwhile, the hobbing process includes cutting time and a relatively short auxiliary time, while the machine feed parts mainly generate heat during the auxiliary time. Thus, the heat generated by the machine guide, ball screw, and other feed systems is relatively small. In addition, we consider the limitations of conducting thermal effect studies only for a single spindle in the dry hobbing machine. Therefore, this study focuses on the thermal accumulation problem of the hob spindle and workbench spindle with cutting heat and bearing heat generation as the primary heat sources and conducts the synergistic optimization study.

3 Quantitative analysis of the spindle thermal energy

3.1 Thermal accumulation model for hob spindle

The heat flow characteristics of hob spindle include the frictional heat generated by the bearings at both ends Q_{hsb}, the cutting heat Q_{hsc}, the forced convective heat exchange between the cooling air to hob and bearings Q_{hshca}, Q_{hsbca}, the convective heat exchange between the air to hob spindle Q_{hsa}, the heat conduction between the hob spindle to the parts in direct contact Q_{hsp}, and the radiation heat exchange between the hob spindle to the surrounding environment Q_{hse}. In addition, the thermal impact of the electronic parts on the machine spindles is relatively small and is ignored. Therefore, the heat flow model of hob spindle is shown in Fig. 4.

In summary, the thermal accumulation Q_{hs} of hob spindle can be expressed as Eq. (1).

$$Q_{hs} = Q_{hsb} + Q_{hsc} - Q_{hshca} - Q_{hsbca} - Q_{hsa} - Q_{hsp} - Q_{hse} \tag{1}$$

Bearing heat generation is calculated by the following equation:

$$Q_{hsb} = \int_0^{t_{hs}} 1.047 \times 10^{-4} M_{hsb} n_h N_{hs} dt \tag{2}$$

where t_{hs} is the total hob rotation time, s; n_h is the hob spindle speed, r/min; N_{hs} is the number of bearings in hob spindle; M_{hsb} is the total friction torque of bearings in the hob spindle, N·mm.

The cutting heat generated during the hobbing process is mainly distributed among chips, cooling air, hob, and workpiece. Part of the cutting heat carried by the workpiece is transferred to the workbench spindle by heat conduction. This study defines the proportion of cutting heat transferred to the hob as R_{hs} and the proportion of cutting heat transferred to the workbench spindle through the workpiece as R_{ws}. Thus, the cutting heat to which the hob spindle is subjected is

Fig. 4 Heat flow model of the hob spindle
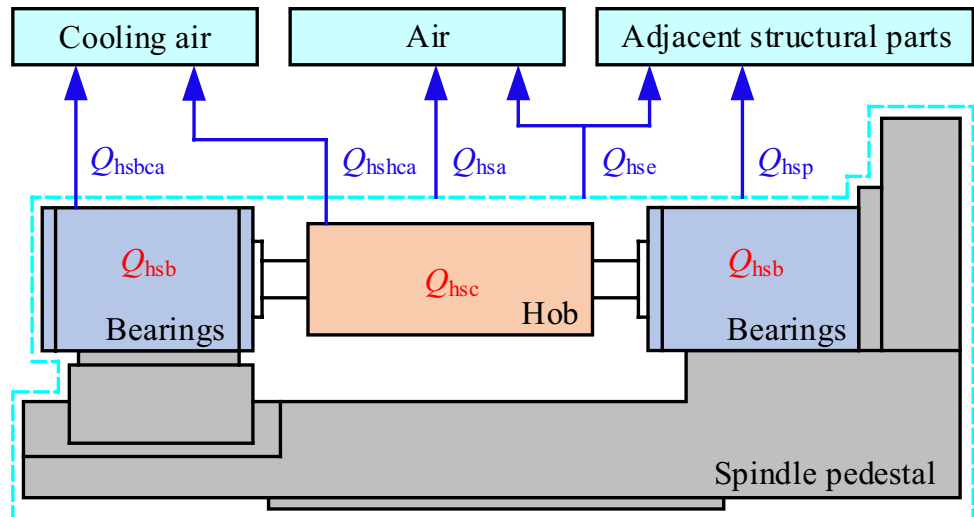
$$Q_{hsc} = \int_0^{t_c} R_{hs} F_c \frac{\pi d_h n_h}{60} dt \tag{3}$$

where t_c is the total cutting time of hob, s.

The heat removed from the hob by cooling air is

$$Q_{hshca} = \int_0^{t_c} \overline{h_h} S_h (T_h - T_c) dt \tag{4}$$

The heat transfer between the bearing of hob spindle and the cooling air is

$$Q_{hsbca} = \int_0^{t_{hs}} h_{hsb} S_{hsb} N_{hs} (T_{hsb} - T_c) dt \tag{5}$$

where $\overline{h_h}$ is the average forced convection heat transfer coefficient, W/(m²·K); T_h, T_c are the temperatures of the hob and cooling air, respectively, °C; S_h is the cooling area of hob (related to the width of flat port nozzle), m²; h_{hsb} is forced convective heat transfer coefficient between the bearings of hob spindle and cooling air, W/(m²·K); S_{hsb} is the convective heat transfer area of bearing in hob spindle, m²; T_{hsb} is the temperature of bearing in hob spindle, °C.

The convective heat transfer of air to the hob spindle is

$$Q_{hsa} = \int_0^{t_t} h_a S_{hs} (T_{hs} - T_a) dt \tag{6}$$

where t_t is the total working time of machine tool, s; h_a is the natural convection coefficient of air, W/(m²·K); S_{hs} is the surface area of hob spindle, m²; T_{hs} is the temperature of hob spindle, °C; T_a is the air temperature, °C.

The heat exchanged by heat conduction between the hob spindle and the adjacent parts is

$$Q_{hsp} = \int_0^{t_t} \lambda_{hsp} \frac{(T_{hs} - T_{hsp})}{\delta_{hsp}} S_{hsp} dt \tag{7}$$

where λ_{hsp} is the thermal conductivity of the adjacent parts for hob spindle, W/(m·K); T_{hsp} is the temperature of adjacent parts, °C; δ_{hsp} is the thickness of adjacent parts, m; S_{hsp} is the area of hob spindle in contact with the adjacent parts, m².

The heat exchanged between the hob spindle and the surrounding environment through heat radiation is

$$Q_{hse} = \int_0^{t_t} \varepsilon_{hs} \sigma S_{hs} (T_{hs} - T_a)^4 dt \tag{8}$$

where ε_{hs} is the emissivity of hob spindle; σ is the Stephen-Boltzmann constant, $\sigma = 5.67 \times 10^{-8}$ W/(m²·K⁴).

Thus, the thermal accumulation Q_{hs} of the hob spindle can be further expressed as

$$Q_{hs} = Q_{hsb} + Q_{hsc} - Q_{hshca} - Q_{hsbca} - Q_{hsa} - Q_{hsp} - Q_{hse}$$

$$= \begin{pmatrix} \int_0^{t_{hs}} 1.047 \times 10^{-4} M_{hsb} n_h N_{hs} dt + \int_0^{t_c} R_{hs} F_c \frac{\pi d_h n_h}{60} dt - \\ \int_0^{t_c} \overline{h_h} S_h (T_h - T_c) dt - \int_0^{t_{hs}} h_{hsb} S_{hsb} N_{hs} (T_{hsb} - T_c) dt - \\ \int_0^{t_t} h_a S_{hs} (T_{hs} - T_a) dt - \int_0^{t_t} \lambda_{hsp} \frac{(T_{hs} - T_{hsp})}{\delta_{hsp}} S_{hsp} dt - \\ \int_0^{t_t} \varepsilon_{hs} \sigma S_{hs} (T_{hs} - T_a)^4 dt \end{pmatrix} \tag{9}$$

3.2 Thermal accumulation model for workbench spindle

The heat flow characteristics of the workbench spindle in dry hobbing machine include the frictional heat generated by bearings Q_{wsb}, the cutting heat Q_{wsc}, the heat transferred

by hot chips falling onto the workbench spindle Q_{wshc}, the forced convective heat transfer between the cooling air and bearings Q_{wsbca}, the convective heat transfer between the air and workbench spindle Q_{wsa}, the heat conduction between the workbench spindle to the parts in direct contact Q_{wsp}, and the radiation heat transfer between the workbench spindle to the surrounding environment Q_{wse}, as shown in Fig. 5.

Therefore, the heat accumulation Q_{ws} of the workbench spindle can be expressed as Eq. (10).

$$Q_{ws} = Q_{wsb} + Q_{wsc} + Q_{wshc} - Q_{wsbca} - Q_{wsa} - Q_{wsp} - Q_{wse} \tag{10}$$

There are two groups of bearings inside the workbench spindle in dry hobbing machine, and the bearings are located at the upper and lower ends of workbench spindle. Therefore, the thermal generated by bearings inside the workbench spindle can be calculated using the following equation:

$$Q_{wsb} = \int_0^{t_{ws}} 1.047 \times 10^{-4} M_{wsb} n_w N_{ws} dt \tag{11}$$

where N_{ws} is the number of bearings in the workbench spindle; t_{ws} is the total workbench spindle rotation time, s; M_{wsb} is the total friction torque of bearings, N·mm; n_w is the rotation speed of workbench spindle, r/min.

The cutting heat to which the workbench spindle is subjected is

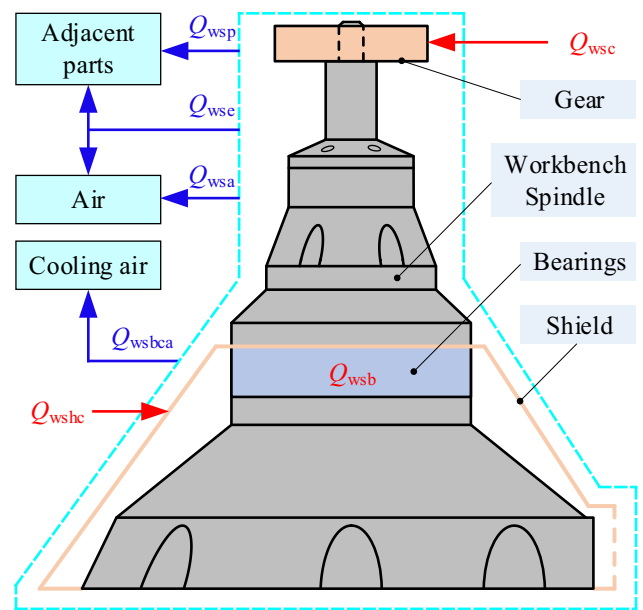$$Q_{wsc} = \int_0^{t_c} R_{ws} F_c \frac{\pi d_h n_h}{60} dt \tag{12}$$

The heat transfer from the hot chips to workbench spindle is [20]

$$Q_{wshc} = n \lambda_s l_r e_w \frac{T_{hc} - T_{ws}}{\delta_s} t_r \tag{13}$$

where n is the total number of chips; λ_s is the thermal conductivity of workbench shield, W/(m·°C); l_r is the length of chip rolling down on the shield, m; e_w is the contact width between the chip and shield, m; T_{hc} is the hot chip temperature, °C; T_{ws} is the workbench spindle temperature, °C; δ_s is the shield thickness, m; and t_r is chip rolling down time on workbench spindle, s.

The heat exchange between the bearing inside workbench spindle and cooling air is

$$Q_{wsbca} = \int_0^{t_{ws}} h_{wsb} S_{wsb} N_{ws} (T_{wsb} - T_c) dt \tag{14}$$

where h_{wsb} is the forced convective heat transfer coefficient between the bearings inside workbench spindle and cooling air, W/(m²·K); S_{wsb} is the convective heat transfer area of bearings inside the workbench spindle, m²; T_{wsb} is the temperature of bearings inside the workbench spindle, °C.

The convective heat exchange between the air and the workbench spindle is

$$Q_{wsa} = \int_0^{t_t} h_a S_{ws} (T_{ws} - T_a) dt \tag{15}$$

where S_{ws} is the surface area of workbench spindle, m².

The heat exchanged by heat conduction between the workbench spindle and adjacent parts is

$$Q_{wsp} = \int_0^{t_t} \lambda_{wsp} \frac{(T_{ws} - T_{wsp})}{\delta_{wsp}} S_{wsp} dt \tag{16}$$

where λ_{wsp} is the thermal conductivity of adjacent parts for the workbench spindle, W/(m·K); T_{wsp} is the adjacent part temperature of workbench spindle, °C; δ_{wsp} is the adjacent part thickness of workbench spindle, m; S_{wsp} is the area of workbench spindle in contact with adjacent parts, m².

The heat exchange of workbench spindle to the surrounding environment through heat radiation is

$$Q_{wse} = \int_0^{t_t} \varepsilon_{ws} \sigma S_{ws} (T_{ws} - T_a)^4 dt \tag{17}$$

where ε_{ws} is the emissivity of workbench spindle.

In summary, the heat accumulation Q_{ws} of the workbench spindle can be further expressed as

Fig. 5 Heat flow model of the workbench spindle

$$Q_{ws} = Q_{wsb} + Q_{wsc} + Q_{wshc} - Q_{wsbca} - Q_{wsa} - Q_{wsp} - Q_{wse}$$

$$= \begin{pmatrix} \int_0^{t_{ws}} 1.047 \times 10^{-4} M_{wsb} n_w N_{ws} dt + \int_0^{t_c} R_{ws} F_c \frac{\pi d_h n_h}{60} dt + \\ n\lambda_s l_r e_w \frac{T_{hc} - T_{ws}}{\delta_s} t_r - \int_0^{t_{ws}} h_{wsb} S_{wsb} N_{ws} (T_{wsb} - T_c) dt - \\ \int_0^{t_t} h_a S_{ws} (T_{ws} - T_a) dt - \int_0^{t_t} \lambda_{wsp} \frac{(T_{ws} - T_{wsp})}{\delta_{wsp}} S_{wsp} dt - \\ \int_0^{t_t} \varepsilon_{ws} \sigma S_{ws} (T_{ws} - T_a)^4 dt \end{pmatrix}$$

$$(18)$$

3.3 Characteristic parameters calculation for thermal accumulation models

According to the analysis in Section 2, cutting heat and bearing frictional heat generation are the leading causes of thermal accumulation in hob spindle and workbench spindle. Meanwhile, during the dry hobbing process, the hob spindle and workbench spindle are subject to convective heat exchange with the air, forced convective heat transfer between the hob and bearings and the cooling air, heat conduction between the hob spindle and workbench spindle and adjacent parts, as well as heat radiation with the surrounding environment. Therefore, the cutting heat generation efficiency P_c, bearing friction heat generation efficiency P_b, bearing and cooling air forced convection heat transfer efficiency P_{bca}, the heat conduction efficiency P_{sp} of the spindles and adjacent parts, and the spindles and the surrounding environment heat radiation efficiency P_{se} are common characteristic parameters of the thermal accumulation model for the hob spindle and workbench spindle, which are calculated as follows.

For cutting heat, the elastic and plastic deformation works of workpiece material and the friction work between the hob-chip and hob-gear are almost entirely converted into cutting heat. Combined with the functional relationship between the cutting line speed and the spindle speed in dry hobbing, the cutting heat production efficiency can be determined according to Eq. (19), where the cutting force F_c can be obtained based on Eq. (20) proposed by the Pfauter Co., Ltd. [15].

$$p_c = F_c \frac{\pi d_h n_h}{60} \tag{19}$$

$$F_c = \frac{1.96 \times 10^4 m^{0.95} f^{0.8} a_p^{0.15} e^{0.012\beta} C_g}{V_c^{0.28} i^{0.7} A^{0.6}} e^{0.65\chi z^{-0.35}} C_w \tag{20}$$

where d_h is the hob diameter, m; m is the gear module, mm; f is the hob axial feed, mm/r; a_p is the hobbing depth, mm; β is the gear helix angle, °; C_g is the hob head coefficient; χ is the gear hob head coefficient, for master gear, $\chi = 0$; z is the tooth numbers of gear; C_w is the gear material coefficient; V_c is hob cutting speed ($V_c = \pi d_h n_h$), m/min; i is the number of hob grooves; A is the hob coefficient, $A = d_h/2 m$.

For the frictional heat generation of bearings, its heat generation efficiency can be calculated by Eq. (21), where the frictional torque is calculated according to Eq. (22) as referenced to Ref. [15].

$$P_b = 1.047 \times 10^{-4} M_{sb} n_{sb} \tag{21}$$

$$M_{sb} = \begin{cases} 10^{-7} f_0 (\nu n_{sb})^{2/3} D_m^3 + f_1 P_1 D_m & \nu n_{sb} \geq 2000 \\ 1.6 \times 10^{-5} f_0 D_m^3 + f_1 P_1 D_m & \nu n_{sb} < 2000 \end{cases} \tag{22}$$

where M_{sb} is the total friction torque of the rolling bearing, N·mm; n_{sb} is the bearing support shaft speed, r/min; f_0 is the coefficient related to the bearing type and lubrication; ν is the kinematic viscosity of the bearing lubricating fluid, mm²/s; D_m is the bearing middle diameter, mm; f_1 is the coefficient related to the bearing structure and load; P_1 is determined by the load on the bearing.

For thermal convection heat transfer, there is forced convection heat transfer between the cooling air and the hob and bearings, and natural convection heat transfer between the air and the hob spindle and workbench spindle, which differ by the convection heat transfer coefficient. Considering the large amount of heat generated during the hobbing process and in order to prevent hot chips from accumulating on the hob, cooling air is used to cool the hob spindle and blow away the chips. Therefore, the hob spindle is subjected to forced convection heat transfer from the cooling air, as shown in Fig. 6. The cooling air is passed through the flat port nozzle to cool hob in the form of impinging jet, and the forced convection heat transfer efficiency P_h can be calculated by Eq. (23) as referenced to Ref. [21].

$$P_h = \overline{h_h} S_h (T_h - T_c) \tag{23}$$

$$\begin{cases} \overline{h_h} = \frac{k\overline{Nu}}{D_h} \\ \overline{Nu} = \frac{3.06}{x/W + H/W + 2.78} Re^{m_c} Pr^{0.42} \\ m_c = 0.695 - \left[\left(\frac{x}{2W} \right) + \left(\frac{H}{2W} \right)^{1.33} + 3.06 \right]^{-1} \\ Re = \frac{V_{ca} D_h}{\nu_{ca}} \end{cases} \tag{24}$$

where k is the thermal conductivity of cooling air, W/(m·K); $\overline{Nu}$ is the average Nussle number; D_h is the characteristic length, m; W is the nozzle slit width, m; H is the distance between the nozzle and hob surface, m; Re is the Reynolds number; Pr is the Prandtl number; V_{ca} is the flow speed of cooling air, m/s; ν_{ca} is the kinematic viscosity of cooling air, m²/s, where the functional relationship between the kinematic viscosity of cooling air and its temperature is $\nu_{ca} = 8 \times 10^{-11} T_c^2 + 9 \times 10^{-8} T_c + 2 \times 10^{-5}$.

Fig. 6 Forced heat exchange principle of hob
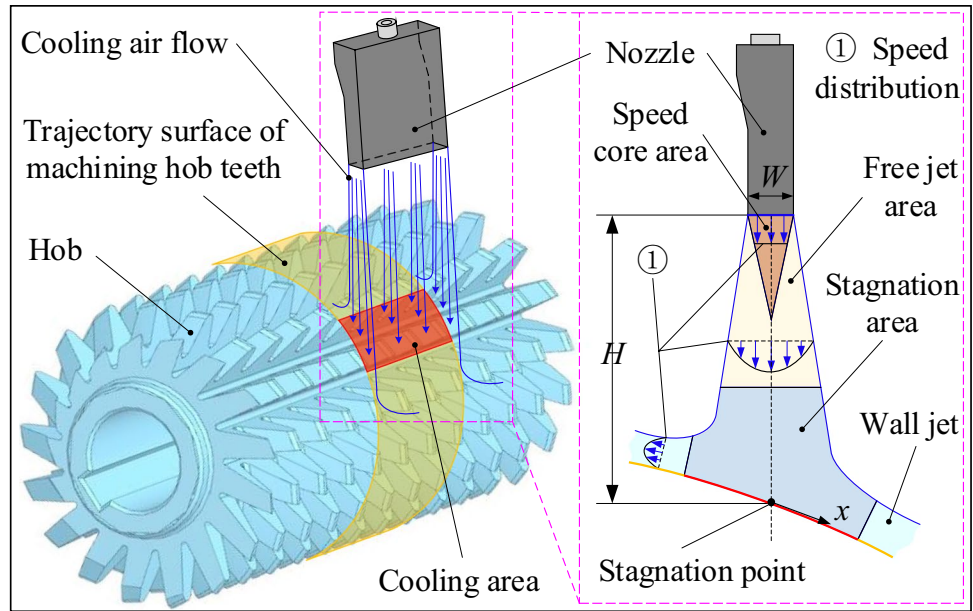
For forced convection transfer between the bearing and cooling air, the forced convection heat transfer efficiency P_{bca} can be calculated by Eq. (25) as referenced to Ref. [17].

$$P_{bca} = h_{sb}S_{sb}(T_{sb} - T_c) \tag{25}$$

$$h_{sb} = \frac{0.0266kPr^{1/3}(\rho V_{sbca})^{0.805}}{d_m^{0.195}v_{ca}^{0.805}} \tag{26}$$

where h_{sb} is the forced convective heat transfer coefficient of the cooling air to bearing, W/(m²·K); S_{sb} is the convective heat transfer area of bearing, m²; T_{sb} is the bearing temperature, °C; ρ is the air density, kg/m³; V_{sbca} is the flow speed of cooling air in the bearing, m/s; d_m is the bearing middle diameter, m, where the average flow speed of the cooling air in the bearing, V_{sbca}, can be calculated by Eq. (27).

$$V_{sbca} = \frac{\pi n_b d_m S_{sb}}{60(S_{sb}^2 - 1)^{1/2}} \tag{27}$$

For the heat conduction transfer of machine spindles, as this study focuses on the thermal accumulation effect of the hob spindle and workbench spindle on their thermal deformation, only the heat conduction between the hob spindle and workbench spindle and adjacent parts is considered, and the specific heat conduction efficiency can be calculated by the following equation:

$$P_{sp} = \lambda_{sp} \frac{(T_s - T_{sp})}{\delta_{sp}} S_{sp} \tag{28}$$

where P_{sp} is the heat conduction efficiency, W; λ_{sp} is the thermal conductivity of adjacent parts, W/(m·K); T_s is the temperature of the hob spindle or workbench spindle, °C; T_{sp} is the temperature of the adjacent parts of the hob spindle or workbench spindle, °C; δ_{sp} is the thickness of the adjacent parts of the hob spindle or workbench spindle, m; S_{sp} is the area of the hob spindle or workbench spindle in contact with the adjacent parts, m².

For heat radiation transfer between the machine spindles and the surrounding environment, in the cutting space, heat transfer by heat radiation occurs mainly on the component surface and in the air. The radiative heat transfer efficiency can be calculated from Eq. (29) as referenced to Ref. [21].

$$P_{se} = \varepsilon_s \sigma S_s (T_s - T_a)^4 \tag{29}$$

where P_{se} is the radiation heat transfer efficiency, W; ε_s is the emissivity; S_s is the surface area of the hob spindle or workbench spindle, m².

4 Multi-objective optimization approach for minimum spindle thermal accumulation

4.1 Multi-objective optimization model

The hob spindle and workbench spindle in dry hobbing machine are key components in direct contact with the workpiece, and their temperature field distribution characteristics and thermal deformation directly affect the gear machining quality. Thermal accumulation is a decisive factor in the temperature rise of the machine spindles. Therefore, this study takes the optimization objective for the minimum thermal accumulation of the hob spindle and workbench spindle.

Combined with the heat transfer calculation equations for heat conduction and heat radiation, on the one hand, considering that the temperature change between the hob spindle and workbench spindle and the contact position of adjacent parts is relatively tiny; on the other hand, the temperature difference between the hob spindle and workbench spindle and the cutting space is not significant, and the Stephen-Boltzmann constant σ is of order 10^{-8}; the heat exchange of the hob spindle and workbench spindle through heat conduction and heat radiation is ignored. Therefore, the optimization objectives can be further expressed as Eqs. (30) and (31).

$$
\begin{aligned}
Q_{hs} &= Q_{hsb} + Q_{hsc} - Q_{hshca} - Q_{hsbca} - Q_{hsa} \\
&= \begin{pmatrix} \int_0^{t_{hs}} 1.047 \times 10^{-4} M_{hsb} n_h N_{hs} dt + \int_0^{t_c} R_{hs} F_c \frac{\pi d_h n_h}{60} dt - \\ \int_0^{t_c} \overline{h_h} S_h (T_h - T_c) dt - \int_0^{t_{hs}} h_{hsb} S_{hsb} N_{hs} (T_{hsb} - T_c) dt - \\ \int_0^{t_t} h_a S_{hs} (T_{hs} - T_a) dt \end{pmatrix}
\end{aligned}
$$
(30)

$$
\begin{aligned}
Q_{ws} &= Q_{wsb} + Q_{wsc} + Q_{wshc} - Q_{wsbca} - Q_{wsa} \\
&= \begin{pmatrix} \int_0^{t_{ws}} 1.047 \times 10^{-4} M_{wsb} n_w N_{ws} dt + \int_0^{t_c} R_{ws} F_c \frac{\pi d_h n_h}{60} dt + \\ n\lambda_s l_r e_w \frac{T_{hc} - T_{ws}}{\delta_s} t_r - \int_0^{t_{ws}} h_{wsb} S_{wsb} N_{ws} (T_{wsb} - T_c) dt - \\ \int_0^{t_t} h_a S_{ws} (T_{ws} - T_a) dt \end{pmatrix}
\end{aligned}
$$
(31)

The dry hobbing process includes cutting time and auxiliary time such as loading and unloading. The auxiliary time mainly depends on the automation degree of the machine. Cutting time is mainly related to the cutting speed, feed, and other process parameters, directly affecting the hobbing machining efficiency. Therefore, there is some constraint between machining efficiency and the thermal accumulation of the hob spindle and workbench spindle. To optimize the thermal accumulation of the hob spindle and workbench spindle without reducing machining efficiency, cutting time is used to represent machining efficiency, which is considered an optimization objective. The cutting time is the ratio of axial travel to axial feed speed. The axial travel contains the approach safety tolerance, the retract safety tolerance, the approach travel, and the overstep travel. Based on engineering experience, the approach safety tolerance and the retract safety tolerance are both taken as 2 mm. Therefore, the cutting time of gear machining can be calculated by Eq. (32) as referenced to Ref. [17].

$$
t_{cut} = \frac{L_{pt} + L_{bt} + B + 4}{n_h f N_h / z}
$$
(32)

$$
L_{pt} = \begin{cases} \sqrt{d_h \times a_p} & \text{(spur gear)} \\ \sqrt{a_p \times [(d_h + d_w)\tan^2\delta + d_h]} & \text{(helix gear)} \end{cases}
$$
(33)

$$
L_{bt} = 1.25 m \sin\delta / \tan\alpha_n
$$
(34)

where t_{cut} is the cutting time, min; L_{pt} is the approach stroke, mm; L_{bt} is the overstep travel, mm; B is the workpiece width, mm; N_h is the number of hob heads; d_w is the outside diameter of workpiece, mm; δ is the installation angle of hob, °; α_n is the normal pressure angle of workpiece, °.

For decision variables, during the dry hobbing process, the ratio of workbench spindle rotation speed to hob speed is equal to the ratio of hob head number to the tooth numbers, which are closely related to the heat generation of the bearings in hob spindle and workbench spindle. The speed and axial feed of the hob are essential factors influencing the cutting heat. Meanwhile, the hob speed is related to the heat transfer from the hot chips to workbench spindle. For heat dissipation in cutting space, the relevant parameters of the cooling air are controllable factors in determining heat dissipation. Therefore, three decision variables are considered for optimizing the thermal accumulation in the hob spindle and workbench spindle, i.e., $n_h, f,$ and T_c.

For constraint conditions, to ensure that the dry hobbing machine works appropriately, the optimized parameters should be within the performance and process requirements of the machine. According to the technical manual for the dry hobbing machine, the value range of speed and axial feed for hob and the temperature of cooling air can be obtained.

$$
n_{h,min} \leq n_h \leq n_{h,max}
$$
(35)

$$
f_{min} \leq f \leq f_{max}
$$
(36)

$$
T_{c,min} \leq T_c \leq T_{air}
$$
(37)

where $n_{h,max}, n_{h,min}$ are the maximum and minimum values of spindle speed; f_{min}, f_{max} are the maximum and minimum values of hob axial feed; $T_{c,min}$ is the minimum value of cooling air temperature.

Based on the above analysis, a multi-objective optimization model of dry hobbing machine process parameters with synergistic optimization for hob spindle thermal accumulation Q_{hs} and workbench spindle heat accumulation Q_{ws} is established while maximizing machining efficiency t_{cut}, i.e.,

$$
F(n_h, f, T_c) = (\min Q_{hs}, \min Q_{ws}, \min t_{cut})
$$
$$
s.t. \begin{cases} n_{h,min} \leq n_h \leq n_{h,max} \\ f_{min} \leq f \leq f_{max} \\ T_{c,min} \leq T_c \leq T_{air} \end{cases}
$$
(38)

4.2 Intelligent solution method for optimization model

In this study, intelligent algorithms are used to optimize the hobbing process parameters to reduce the thermal accumulation in the hob spindle and workbench spindle. Also, the workpiece machining efficiency is balanced while minimizing the heat accumulation in the hob spindle and workbench spindle. Therefore, this study needs to solve a triple objective optimization problem. NSGA-III is a suitable optimization algorithm for solving more than two objectives [22]. NSGA-III achieves a more remarkable improvement in the ranking of congestion degree compared to NSGA-II, which mainly introduces widely distributed reference points to maintain population diversity, making it quite effective in solving high-dimensional objectives. The optimization process of the algorithm NSGA-III for dry hobbing process parameters is shown in Fig. 7.

Step 1: Coding and initialization of populations. The parameters involved in the algorithm are encoded in real coding, and an initial parent population P_t of size N is randomly generated based on the range of speed and axial feed for the hob and the temperature of cooling air.

Step 2: Generate offspring populations. The initial parent population P_t is substituted into Eqs. (30)–(32) to obtain the fitness value of each individual. The aim of this study is to solve for the minimum thermal accumulation for the hob spindle and workbench spindle as well as the minimum cutting time. Therefore, the individuals are fast non-dominated sorted, normalized, and associated with reference points according to the minimum fitness value. Then, the initial population is selected, crossed, and varied to produce progeny populations Q_t of size N.

Step 3: Merge populations and generate new parent populations. The parent and offspring populations are merged into a population of size $2N$, then fast non-dominated sorted, normalized, and associated with reference points according to the minimum thermal accumulation of the hob spindle and workbench spindle as well as the minimum cutting time, followed by crowding calculation. N individuals are selected from the merged population to create a new parent population R_t by fast non-dominated sorting.

Fig. 7 Solving process of thermal accumulation optimization model
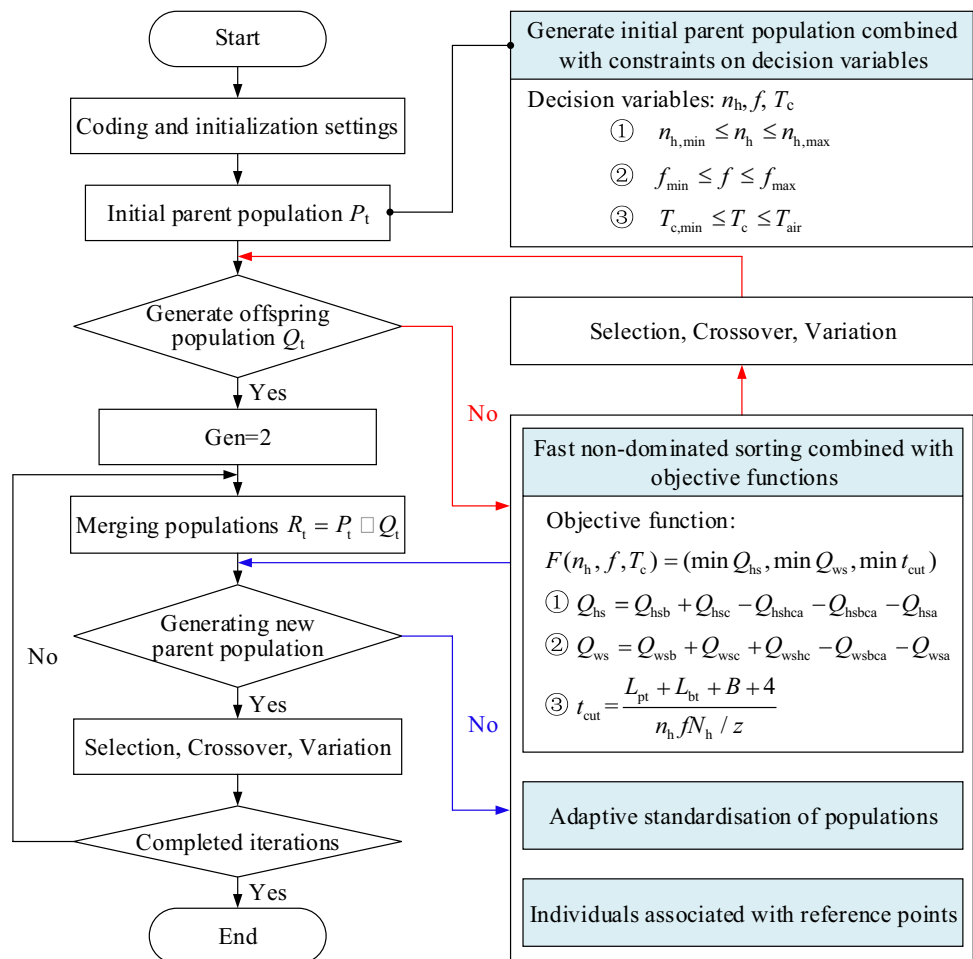
Step 4: Determine whether the algorithm reaches the termination condition. If the population does not get the iteration termination condition, go to step 2.

5　Case study

The dry hobbing cylindrical spur gear is taken as an example to solve and validate the optimization model in this study. Based on the performance of dry hobbing machine and actual processing condition, the hob speed is set in the range of 500–1500 r/min, the hob axial feed is 1–3 mm/r, and the cooling air temperature is taken to be 5–25 °C. For the main parameters of workpiece, the normal modulus of gear (m) is 2 mm, the tooth number (z) is 31, the gear material coefficient (C_w) is 1.34, the gear outside diameter (d_w) is 70.49 mm, the gear width (B) is 13 mm, and the gear normal pressure angle (α_n) is 20°. For the main parameters of hob, the outside diameter of hob (d_h) is 70 m, the number of hob heads (N_h) is 3, the hob head coefficient (C_g) is 2, the number of hob grooves (i) is 17, and the hob installation angle (δ) is 5°19′. For the process parameters of hobbing, the cutting depth (a_p) is 4.5 mm and the flow speed of cooling air (V_{cool}) is 313 m/s.

5.1　Optimization results

Based on the above dry hobbing data, the established optimization model is solved by the algorithm NSGA-III. Figure 8 shows the multi-objective optimization solution set obtained by the algorithm NSGA-III. As shown in Fig. 8, point C is the theoretical optimum solution, where the thermal accumulation of hob spindle and workbench spindle as well as cutting time are minimized. In contrast, point D results in maximum hob spindle and workbench spindle thermal accumulation and cutting time. Also, as shown in Fig. 8, the thermal accumulation of both the hob spindle and workbench spindle at point A is minimal, and the cutting time is large, reducing the workpiece's production efficiency. The cutting time at point B is minimal, and yet the thermal accumulation of the hob spindle and workbench spindle becomes larger, which will lead to severe thermal deformation of the hob spindle and workbench spindle.

Based on the above optimal solution selection problem for the Pareto, this study adopts the entropy weight TOPSIS synthetic decision method for optimal solution selection [23]. Firstly, the Pareto data is reversed and normalized; then, the entropy weighting method is used to analyze the thermal accumulation of the hob spindle and workbench spindle as well as the machining efficiency; finally, TOPSIS is adopted to calculate the comprehensive ranking of each index. The final trade-off optimal solution for thermal accumulation of the hob spindle and workbench spindle as

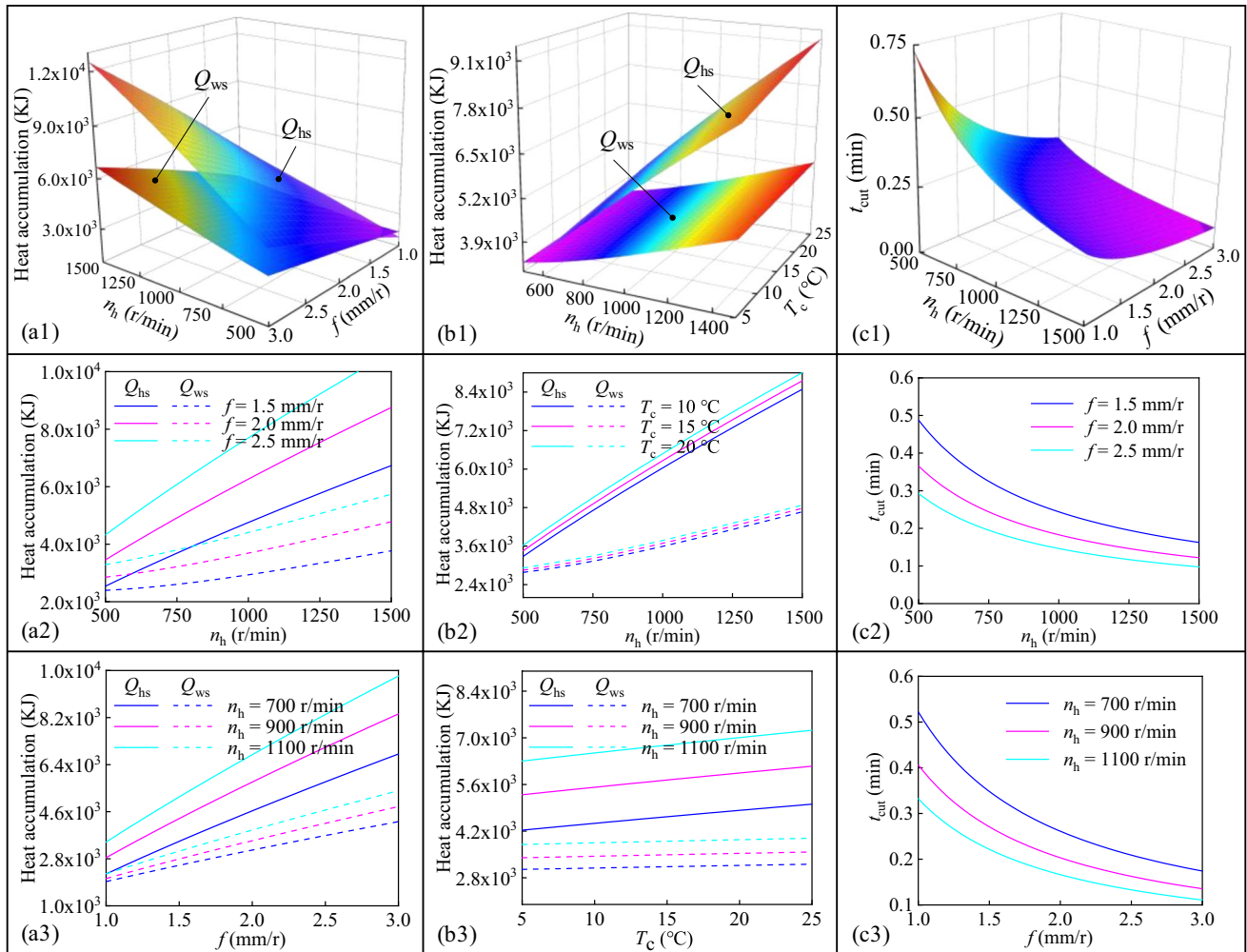**Fig. 8** Pareto solution sets for multi-objective optimization
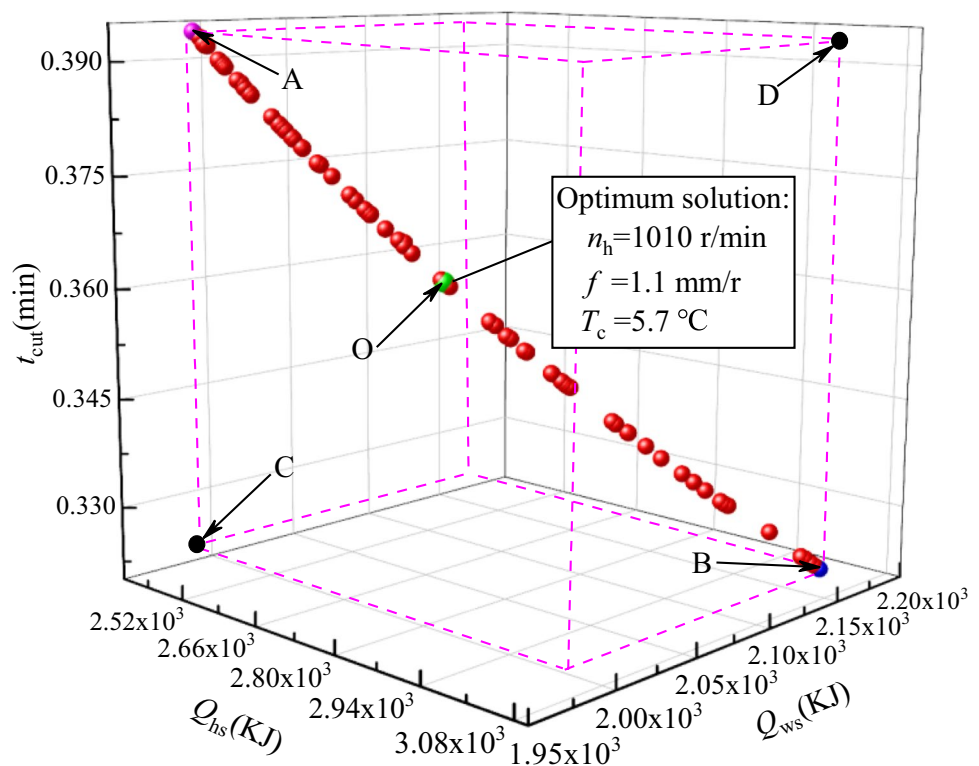
Fig. 9 The impacts of decision variables on Q_{hs}, Q_{ws}, and t_{cut}

well as the machining efficiency is obtained, where the hob speed n_h is 1010 r/min, the hob axial feed f is 1.1 mm/r, and the cooling air temperature T_c is 5.7 °C.

To investigate the impact of decision variables on the thermal accumulation Q_{hs}, Q_{ws} in dry hobbing machine spindles and machining efficiency t_{cut}, sensitivity analysis has been conducted. As shown in Fig. 9a1 and b1, the decision variables have the same impact trend on the thermal accumulation for hob spindle and workbench spindle, and the thermal accumulation of hob spindle is overall higher than the thermal accumulation of workbench spindle. It is caused by the fact that the hob spindle speed is higher than the workbench spindle speed, resulting in greater heat generation from the bearings within the hob spindle; in addition, the heat transferred from cutting heat into the workbench spindle is carried away partly by the workpiece. As shown in Fig. 9a2, a3, b2, and b3, the thermal accumulations Q_{hs}, Q_{ws} of the dry hobbing machine spindles increase with the increase in hob speed/axial feed/cooling air temperature.

However, higher hob speed and axial feed can reduce machining times, and higher hob speed can increase the forced convection heat transfer coefficient between the bearing and the cooling air, which helps to reduce heat build-up in the machine tool spindle. As shown in Fig. 9c1, c2, and c3, the cutting time t_{cut} increases with increasing hob speed/ axial feed; in addition, the cutting time t_{cut} is an important factor affecting the heat production of the machine spindles and an essential indicator for controlling the gear machining efficiency.

5.2 Experimental validation

To verify the validity of the optimization model, the optimum parameters obtained are verified by experiment on a dry hobbing machine. In this study, the temperature sensor Pt100 is adopted to collect the temperature variations of the brackets at two ends in hob spindle as well as the workbench spindle. The placements of the temperature sensors and the
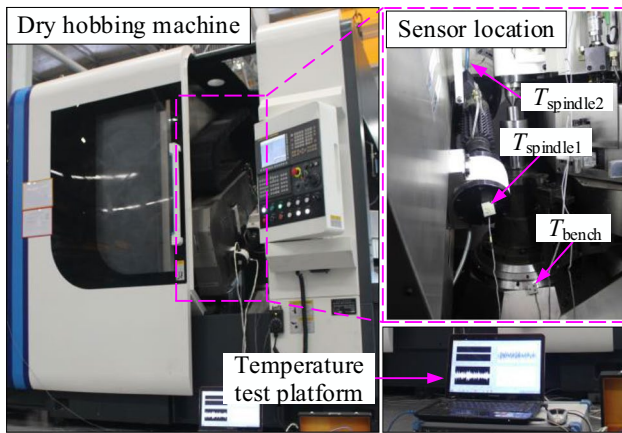
Fig. 10 Experimental setup for temperature testing

machining efficiency while also benefiting the reduction of thermal deformation in machine components. In addition, hobbing experiments were carried out for the before- and after-optimization process parameters. As shown in Fig. 11, during the hobbing process, the temperature at each collection point first undergoes a rapid rise and then gradually stabilizes. After optimizing the parameters, the temperature of each collection point decreased, and the average temperature change of each collection point is shown in Table 1. Therefore, the optimization results effectively reduce the temperature of the hob spindle and workbench spindle in dry hobbing machine and improve the gear machining efficiency.

It is worth emphasizing that the thermal deformation of the dry hobbing machine components is an important factor affecting the gear machining accuracy, especially the thermal deformation of the hob spindle and workbench spindle, which will directly affect the contact position of the hob and workpiece, causing tooth shape error, tooth pitch error, tooth direction error, etc. Therefore, to further verify the optimization model's validity, the workpiece's M-values before and after optimization are measured and compared in this study. As shown in Fig. 12, with the machining time, the thermal

temperature collection platform are shown in Fig. 10. Based on engineering experience, the values of the unoptimized decision variables are as follows: hob speed n_h is 800 r/min, axial feed of the hob f is 1.6 mm/r, and the cooling air temperature T_c is 13 °C.

We compared the values for the decision variables before and after optimization on the machine's thermal accumulation and machining efficiency, respectively. It can be found that after the optimization, the thermal accumulation of hob spindle is reduced from 3.05×10^3 to 2.71×10^3 kJ, the thermal accumulation of workbench spindle is reduced from 2.53×10^3 to 2.04×10^3 kJ, and the cutting time is reduced from 0.394 to 0.361 min, which are reduced by 11.17%, 19.3%, and 8.22%, respectively. It improves the gear

Table 1 Average temperature variation of collection points

Original parameters	Average temperature (°C)	Optimized parameters	Average temperature (°C)	Effects
$T_{spindle1}$	46.67	$T_{spindle1}$	43.24	↓7.35%
$T_{spindle2}$	49.74	$T_{spindle2}$	44.32	↓10.9%
T_{bench}	28.44	T_{bench}	26.28	↓7.59%

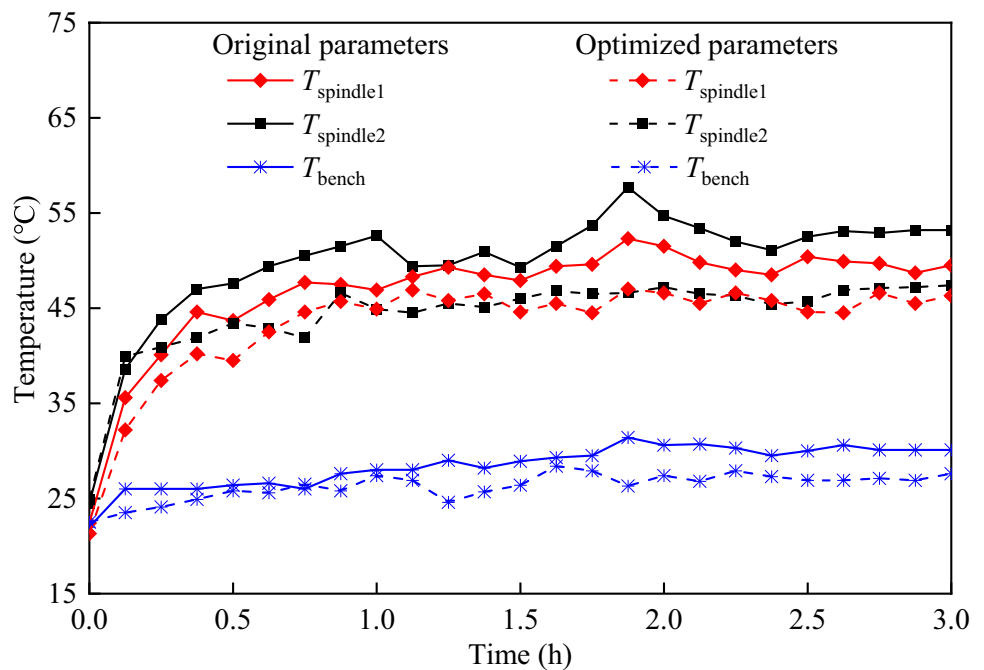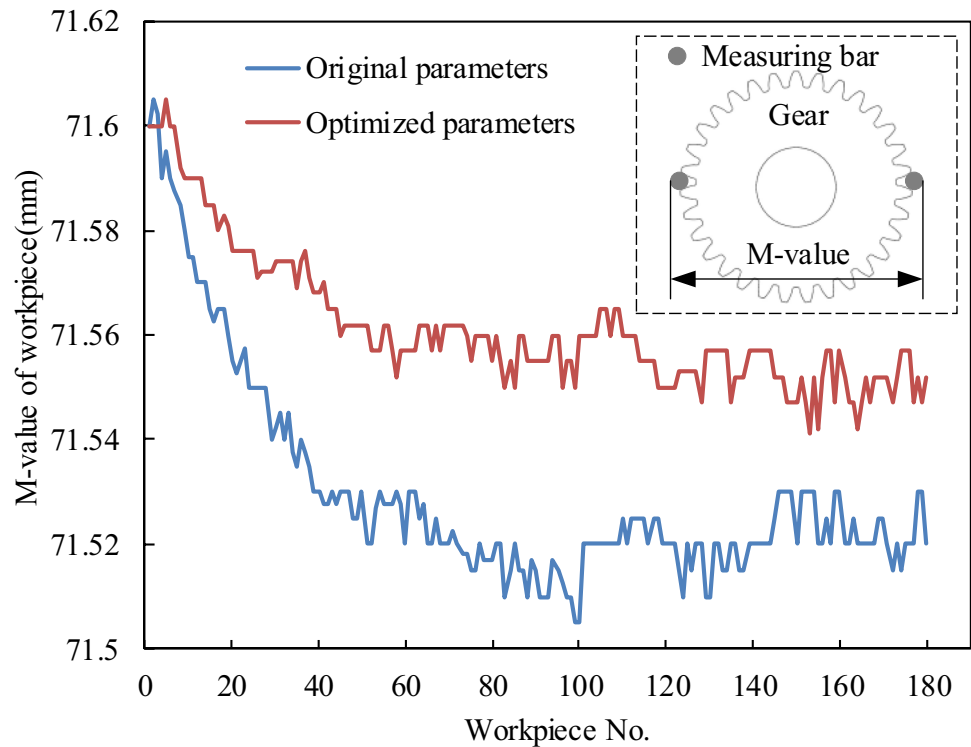**Fig. 11** Temperature change curve of collection point

Fig. 12 M-value variation curve before and after optimization

deformation of the machine spindles gradually increases, leading to a gradual increase in the deviation of the workpiece's M-value, and finally stabilizing, which is consistent with the temperature change of the machine's spindles in Fig. 11. For the original gear machining parameters, the maximum deviation of M-values is 0.095 mm, while with the optimized parameters, the maximum deviation of M-values is reduced to 0.059 mm. The results show that the proposed thermal accumulation optimization model of dry hobbing machine is effective in improving gear machining accuracy.

6 Conclusions

The thermal accumulation of the hob spindle and workbench spindle is directly related to the thermal error for the dry hobbing machine. This study focuses on the thermal accumulation models of the hob spindle and workbench spindle and their optimal control method to reduce the thermal influence of the machine tool and improve the gear machining accuracy. The study results are as follows.

(1) Combined with the analysis of the structure and motion relationship for the hob spindle and workbench spindle, the heat transfer model of dry hobbing machine spindles is established, and the thermal accumulation deformation mechanism of the dry hobbing machine spindles is clarified.

(2) The thermal accumulation calculation models of the dry hobbing machine spindles are established, and the characteristic parameters of the thermal accumulation calculation model are quantitatively analyzed.

(3) A multi-objective optimization approach for process parameters considering the minimum thermal accumulation of the dry hobbing machine spindles is proposed. By applying the proposed optimization method, the thermal accumulation of the hob spindle and workbench spindle is reduced by 11.17% and 19.3%, respectively, the hobbing efficiency is increased by 8.22%, and the average temperature of the spindles is reduced as well as the M-value of the gears is controlled.

This study has currently only explored and improved the impact of process parameters on the thermal accumulation in the dry hobbing machine spindles. In fact, the hobbing process parameters are equally closely related to the thermal deformation of the machine spindles. Therefore, further research can be carried out. A mapping relationship between the process parameters and the machine spindle thermal deformation can be established, and the compensation of thermal deformation errors can be considered along with the optimization of thermal accumulation; secondly, by further combining intelligent sensor systems to implement precise regulation for each heat source of the machine tool.

Data availability The datasets used or analyzed during the current study are available from the corresponding author on reasonable request.

Declarations

Ethical approval Not applicable.

Consent to participate Not applicable.

Consent for publication Yes.

Competing interests The authors declare no competing interests.

References

1. Pawanr S, Garg G, Routroy S (2022) A novel approach to model the energy consumption of machine tools for machining cylindrical parts. J Manuf Process 84:28–42
2. Liu C, He Y, Wang Y, Li Y, Wang S, Wang L, Wang Y (2020) Effects of process parameters on cutting temperature in dry machining of ball screw. ISA Trans 101:493–502
3. Gupta K, Laubscher R, Davim J, Jain N (2016) Recent developments in sustainable manufacturing of gears: a review. J Clean Prod 112:3320–3330
4. Sreejith P, Ngoi B (2000) Dry machining: Machining of the future. J Mater Process Technol 101:287–291
5. Li Z, Wang B, Zhu B, Wang Q, Zhu W (2022) Thermal error modeling of electrical spindle based on optimised ELM with marine predator algorithm. Case Stud Thermal Eng 38:102326
6. Bitar-Nehme E, Mayer J (2018) Modelling and compensation of dominant thermally induced geometric errors using rotary axes' power consumption. CIRP Ann 67:547–550
7. Zhang C, Gao F, Yan L (2017) Thermal error characteristic analysis and modeling for machine tools due to time-varying environmental temperature. Precis Eng 47:231–238
8. Zhao Z, Wang Y, Wang Z, Liu J (2019) Thermal analysis for the large precision EDM machine tool considering the spark energy during long-time processing. J Mech Sci Technol 33:773–782
9. Yao X, Du Z, Ge G, Yang J (2020) Dynamic temperature gradient and unfalsified control approach for machine tool thermal error compensation. J Mech Sci Technol 34:319–331
10. Feng W, Li Z, Gu Q, Yang J (2015) Thermally induced positioning error modelling and compensation based on thermal characteristic analysis. Int J Mach Tools Manuf 93:26–36
11. Wei X, Ye H, Miao E, Pan Q (2022) Thermal error modeling and compensation based on Gaussian process regression for CNC machine tools. Precis Eng 77:65–76
12. Narendra Reddy T, Shanmugaraj V, Vinod P, Gopi Krishna S (2020) Real-time thermal error compensation strategy for precision machine tools. Mater Today: Proc 22:2386–2396
13. Zhu L, Cao H, Zeng D, Yang X, Li B (2017) Multi-variable driving thermal energy control model of dry hobbing machine tool. Int J Adv Manuf Technol 92:259–275
14. Kadashevich I, Beutner M, Karpuschewski B, Halle T (2015) A novel simulation approach to determine thermally induced geometric deviations in dry gear hobbing. Procedia CIRP 31:483–488
15. Li X, Yang Y, Zou Z, Liu Z, Wang L, Tang Q (2019) Critical study on the thermal-structural characteristics of worktable assembly of a dry hobbing machine. Int J Adv Manuf Technol 100:179–188
16. Yang X, Cao H, Li B, Jafar S, Zhu L (2018) A thermal energy balance optimisation model of cutting space enabling environmentally benign dry hobbing. J Clean Prod 172:2323–2335
17. Li B, Cao H, Yang X, Jafar S, Zeng D (2018) Thermal energy balance control model of motorised spindle system enabling high-speed dry hobbing process. J Manuf Process 35:29–39
18. Yang X, Zeng L, Chen P, Du Y, Li B (2022) Complex characteristics and multi-dimensional control strategies of heat flow in dry gear hobbing machines. China Mech Eng 33:623–629
19. Yang X, Chen P (2022) Heat transfer enhancement strategies for eco-friendly dry hobbing considering the heat exchange capacity of chips. Case Stud Therm Eng 29:101716
20. Li B, Yang X, Du Y, He L (2022) Optimisation of chip repose angle in dry hobbing machine considering minimum thermal accumulation on workbench. Int J Adv Manuf Technol 122:1821–1833
21. Incropera F, Dewitt D, Bergman T, Lavine A (2007) Fundamentals of heat and mass transfer. John Wiley & Sons Inc
22. Li Y, Zhou S, Liu J, Tong J, Dang J, Yang F, Ouyang M (2023) Multi-objective optimisation of the Atkinson cycle gasoline engine using NSGA III coupled with support vector machine and back-propagation algorithm. Energy 262:125262
23. Li Z, Luo Z, Wang Y, Fan G, Zhang J (2022) Suitability evaluation system for the shallow geothermal energy implementation in region by entropy weight method and TOPSIS method. Renew Energy 184:564–576